Individual Variability in Human Tibia Lead Concentration

Andrew C. Todd[1], Patrick J. Parsons,[2] Shida Tang,[2] and Erin L. Moshier[1]

[1]Mount Sinai School of Medicine, Department of Community and Preventive Medicine, New York, New York, USA; [2]Wadsworth Center, New York State Department of Health and Department of Environmental Health and Toxicology, School of Public Health, The University at Albany, Albany, New York, USA

Our aims in this study were to determine proximal–distal variability in adult human tibia lead concentration via electrothermal atomization atomic absorption spectrometry (ETAAS) and to determine whether there were any differences between core and surface tibia lead concentrations. We analyzed duplicate core and surface tibia samples for lead at multiple proximal–distal sections on 10 adult human cadaver legs. Dried bone samples were digested in nitric acid using microwave-assisted heating, and lead content was determined by ETAAS with Zeeman background correction. Lead concentrations in nine tibiae (one tibia was excluded because some of the data were compromised) ranged from 3.1 to 27.9 μg lead/g of dry bone. Both core and surface tibia lead concentrations were lower at the proximal and distal ends of the tibia. Surface tibia lead was approximately 5 μg/g greater than core tibia lead in six tibiae with relatively low lead concentration, and 8 μg/g greater in three tibiae with relatively high lead concentration. The difference between core and surface tibia lead was independent of proximal–distal tibia location. We conclude that these nine human tibiae showed a greater surface tibia lead concentration than core tibia lead concentration. This observation has consequences for the noninvasive measurement of tibia lead via K-shell and L-shell X-ray fluorescence. *Key words*: atomic absorption spectrometry, bone lead, lead poisoning. *Environ Health Perspect* 109:1139–1143 (2001). [Online 23 October 2001] *http://ehpnet1.niehs.nih.gov/docs/2001/109p1139-1143todd/abstract.html*

Environmental and occupational exposures to lead continue to be widespread public health concerns and the subjects of much study. Exposure to lead is usually assessed by the measurement of lead in whole blood, but blood lead reflects only recent exposure because the biological residence time of lead in blood is approximately 1 month (*1*). The body's largest repository for lead is the skeleton (*2,3*), wherein the residence time of lead is of the order of years (*1,4*); thus bone lead is a good surrogate for lifetime exposure (*5*).

There are few studies of the distribution of lead in the human skeleton using instrumental analytical methods, such as electrothermal atomization atomic absorption spectrometry (ETAAS). Wittmers et al. (*6*) measured lead concentrations in several human bones, including the tibia, from 134 hospital autopsies. They found no linear relationship between bone lead concentration and the location along the diaphysis. The authors reported bone lead concentrations in micrograms per gram of ashed bone because sample pretreatment included a dry-ashing step in which bone material was oxidized to ash using a muffle furnace. Parsons et al. (*7*) reported lead concentrations in the long bones of lead-dosed animals. They found no clear trend in lead distribution along a single 20-cm bovine tibia. The bone lead data of Parsons et al. (*7*) were reported in micrograms per gram dry weight because dried bone material was digested (wet ashed) in concentrated nitric acid. Conversion of bone lead concentrations based on ash weight into concentrations based on dry weight requires data on the percentage of ash in a given sample. Zong (*8*) reported detailed measurements of lead-dosed goats and found that the lead concentration in some goat tibiae increased toward the proximal and distal ends of the tibia. However, no consistent pattern was found in the few animals studied. One aim of our study was to determine whether adult human tibiae yielded more consistent observations.

Bone can be broadly divided into two types: cortical and trabecular. The midshafts (diaphyses) of long bones tend to be predominantly cortical or compact, while the ends (epiphyses) are characteristically more trabecular or spongy. The percentage by mass of calcium is less in trabecular bone than that in cortical bone (*9*). Lead in bone can be measured noninvasively and *in vivo* using ^{109}Cd-based K-shell X-ray fluorescence (KXRF) (*10*). Results of ^{109}Cd-based KXRF are reported in micrograms of lead per gram of bone mineral because the lead signal is normalized to the signal that arises from elastic scatter of the ^{109}Cd γ-rays off the (principally) calcium and phosphorous in the bone matrix (*11*). It has been reported that the ends of tibiae give higher ^{109}Cd-based KXRF results than the mid-shaft (*12*), probably because of the lower mineral content at the more trabecular ends of the tibia. This behavior might itself be dependent on the exposure history of the subject (environmental or occupational exposure, duration of exposure, and presently exposed or exposed in the past). Another aim of our study was to examine the proximal–distal variation in ETAAS-measured human tibia lead concentration.

Finally, a small number of reports have shown higher bone lead concentrations in the outer surface of bone (*13,14*). This observation has consequences for the interpretation of comparisons between the two *in vivo* bone lead techniques: LXRF, which measures lead within 1–2 mm of the tibia surface, and KXRF, which measures the average lead concentration throughout the entire cross-section of tibia (but weighted primarily from the tibia surface).

Materials and Methods

Bone sample preparation and digestion. We obtained 10 adult legs (nine left and one right, from three females and seven males) from human cadavers donated to medical science in accordance with the Mount Sinai School of Medicine institutional guidelines. The legs, which had previously been separated from the cadaver above the knee, were received intact (i.e., no skin or soft tissue had been removed) and were fixed in formaldehyde. In accordance with institutional confidentiality policies, the age, cause of death, medical history, and occupational history of the subjects were unavailable. Each leg was dissected and overlying tissue removed, exposing the tibia, which was extracted using a Model 810 reciprocating autopsy saw (Stryker, Kalamazoo, MI). The extracted tibiae extended to 10 cm both above and below the proximal–distal (approximate) midpoint of the bone shaft. Bone marrow and soft tissue adhering to the tibiae were removed using a scalpel followed by a bone scraper. Each bone was washed with methanol and then with hydrogen peroxide solution (to remove blood and extraneous tissue deposits); finally, each bone was washed with deionized water. Each bare tibia was divided into nine 2-cm cross-sections using a power tool equipped

with diamond disk blades. A diagram of the sampling protocol is shown in Figure 1. The outer 1–2 mm of superficial bone were removed in several slices per section using the diamond disk saw following the irregular shape of the tibia cross-section. We divided the bone samples into two groups for duplicate measurements of core and surface lead content. One tibia was excluded from the statistical analysis because a laboratory incident during sample preparation compromised some of the lead measurements. (However, inclusion of the limited data from this tibia did not alter the results or conclusions.)

Tibia core and surface bone samples were freeze-dried overnight (VirTis Unitop 200/Freezemobile 6; The Virtis Company, Inc., Gardiner, NY) to remove any residual traces of water (from pretreatment with hydrogen peroxide and deionized water) and so we could report bone lead results based on dry weight. Each core or surface sample was completely "dissolved" in concentrated nitric acid (Instra-Analyzed, trace element grade; J. T. Baker, Phillipsburg, NJ) using a modified procedure based on microwave-assisted heating. This modified procedure

was effective in homogenizing calcified bone material. The homogenization protocol (hereafter called digestion) was validated against National Institute of Science and Technology (NIST, Gaithersburg, MD) Standard Reference Materials (SRM) 1486 bone meal and SRM 1400 bone ash. Validation data are provided in Table 1.

Bone cores (≈1–7 g) were digested in 20 mL HNO_3 using a Model 81D microwave digestion system (MDS) (CEM Corporation, Matthews, NC) equipped with 120-psi Teflon-PFA vessels. We removed the vessels' pressure relief disks to prevent pressurization; this modification permits microwave-assisted heating at atmospheric pressure and reduces the potential for uncontrolled exothermic reactions when biological materials are heated in concentrated HNO_3 with microwave radiation (15). Because the MDS 81D oven can accommodate only 12 vessels, each batch consisted of nine bone core samples, two quality control samples (SRM 1486 and 1400), and one digestion blank. We used an optimized two-step heating program with the Model 81D—15 min at 30% power (180 W) followed by 60 min at 20% power (120 W)—

that produced clear digests. The digestate was further diluted to 40 mL with double deionized water; upon standing, a lipid (fat) layer formed at the surface of some samples. The lipid layer was physically disturbed using a clean plastic pipette tip to permit sampling the clear digest for lead measurements.

Surface materials (≈0.5–2 g) were digested in 10 mL concentrated HNO_3 using a Model 2100 MDS (CEM Corporation). The Model 2100 was equipped with a high-throughput sampling accessory that can accommodate up to 30 standard polypropylene conical sample tubes (50 mL). For this approach, sample tube caps were modified with a small vent hole to prevent internal pressurization and to allow digestion at atmospheric pressure. For each batch of surface materials, two positions were reserved for quality control materials (SRM 1486 and 1400) and one for the digestion blank, leaving 27 positions available for bone samples. An optimized two-step heating program was used: 15 min at 30% power (285 W) followed by 60 min at 20% power (190 W). We did not use the MDS 2100 fiber-optic temperature probe with this application. Digests were diluted to 20 mL with double deionized water. As observed with the core samples, a layer of fat formed with some surface samples.

Lead determination in bone digests. Lead was determined in diluted acid digests by ETAAS, and bone lead concentrations are reported in micrograms per gram dry weight. The accuracy and precision of the ETAAS method have been described elsewhere (16). In brief, we measured lead using a Perkin-Elmer model Z5100 ETAAS instrument equipped with transverse Zeeman-effect background correction (Perkin-Elmer, Norwalk, CT). A Zeeman system is very robust and easily able to correct for background absorption arising from the bone matrix. The reported method detection limit (3σ) is 0.6 µg/g (16). Typical day-to-day precision is < 5%. Accuracy has previously been established to be > 1% on the basis of analyses of NIST SRM 1400 bone ash (9.07 µg/g ash weight) and SRM 1486 bone meal (1.335 µg/g). We used SRM 1400 and SRM 1486 for quality control in this study (Table 1) because they are the only bone reference materials available that have a certified lead content.
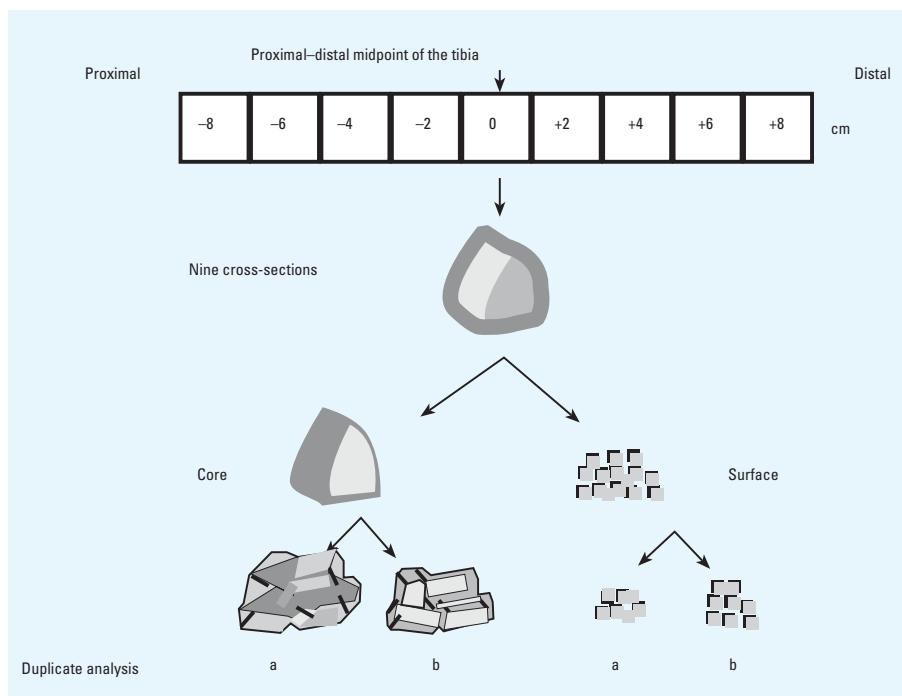

Figure 1. Schematic representation of the sampling protocol.

Table 1. Validation data for bone digestion using microwave-assisted heating at atmospheric pressure coupled with lead determination by ETAAS.

NIST SRM/oven	Mean (µg/g)	SD (µg/g)	RSD	Minimum (µg/g)	Maximum (µg/g)	No.	Certified value[a] (µg/g)
1400 bone ash/CEM 81D	9.2	0.9	9.7%	7.3	10.4	21	9.07 ± 0.12
1400 bone ash/CEM 2100	9.3	0.4	4.7%	8.7	9.9	20	9.07 ± 0.12
1486 bone meal/CEM 81D	1.47	0.21	14.3%	1.11	1.89	21	1.335 ± 0.014
1486 bone meal/CEM 2100	1.48	0.05	3.6%	1.41	1.54	20	1.335 ± 0.014

RSD, relative standard deviation.
[a]SRM uncertainty is defined to be the half-width of the 95% confidence interval for the mean.

Statistical methods. Statistical analyses were performed with SAS software (SAS Institute, Cary, NC). We examined box-plots of average core and surface concentrations (averages were examined instead of the individual duplicates because mixed models with the latter would not converge) for symmetry and any "extreme" outliers (an observation more than three interquartile ranges from the 25th or 75th percentiles). Because there were no extreme outliers, all data were therefore retained and are included in the results. We used the Kolmogorov-Smirnov test to assess normality and Levene's test to assess the homogeneity of variances of the core and surface concentrations obtained at each of the nine proximal–distal locations.

We performed variance component analysis using restricted maximum likelihood estimation (*17*). Both core and surface lead concentrations were modeled as quadratic functions of proximal–distal location, and equations for comparing average core and surface concentrations among tibiae with high and low lead concentrations were estimated using growth curve analysis (*18*) to account for the correlation between measurements made within the same tibia. (The tibiae fell into two groups of relatively high and relatively low lead concentrations.) Akaike's Information Criterion and Schwarz's Bayesian Criterion (*17*) were used to determine which covariance structure best fit the data.

We compared the trends in average atomic absorption spectrometry (AAS) core and surface concentrations over proximal–distal locations among tibiae with both high and low lead concentrations, giving four equations (both core and surface for both high and low lead concentration tibiae). We also tested equality of both the linear and the quadratic location term coefficients of the four equations. When the linear location term coefficients were not significantly different, the four equations were estimated with equal linear location term coefficients. Similarly, when the quadratic location term coefficients were not significantly different,

the four equations were estimated with equal quadratic location term coefficients. Group comparisons were Tukey-adjusted to prevent the inflation of the Type I error rate that is introduced by multiple comparisons.

We looked for contiguous inhomogeneity ("hot spots") in the distribution of lead in the tibiae by calculating the extreme studentized deviate of the differences between the tibia lead concentrations at adjacent locations via a test of the highest and the lowest differences (*19*) and via Grubb's procedure (*20*), a test of the largest differences of either sign.

Results

Analytical issues. Table 1 shows data for the two NIST SRMs analyzed using the two different microwave digestion systems. There was no significant difference between the two microwave digestion procedures (CEM 81D and CEM 2100 with the high throughput accessory). There was good agreement between values found by ETAAS and the certified value for SRM 1400 bone ash (9.07 μg/g), but for SRM 1486 bone meal (1.335 μg/g), there was a small but statistically significant positive bias ($p < 0.004$) for both the CEM 81D (1.47 μg/g) and CEM 2100 (1.48 μg/g) microwave digestion procedures. This small bias (< 0.2 μg/g) is analytically insignificant, if not statistically insignificant, given that the certified lead concentration of SRM 1486 is close to the ETAAS method detection limit. Interestingly, the precision of the Model 2100 with the high throughput accessory is much better than the older Model 81D MDS (for both bone ash and bone meal; F-test p-value < 0.001). Nevertheless, the absence of a significant difference between values found for NIST SRMs using the two microwave digestion systems, coupled with reasonable agreement between found and certified values, provides adequate validation of the modified procedure as a homogenization tool.

Table 2 shows the mean of duplicate ETAAS measurements of tibia core and surface lead concentrations made at the midpoint and at the ends of the dissected tibia

cross-sections. Standard deviations (SD) of the duplicates are not shown because of a lack of robustness based on $n = 2$; however, the precision and reproducibility of the technique have been rigorously quantified elsewhere (*16*). Agreement between the duplicates is addressed in the variance component analysis.

Variance component analysis of ETAAS measurements. Variance component analysis was performed on the duplicate measurements of core and surface concentrations separately to determine the sources of variability for all nine tibiae. The variability (SD) of core concentrations attributable to proximal–distal location was 0.9 μg/g ($p < 0.0001$) and that attributable to tibiae was 4.7 μg/g ($p < 0.0001$). The variability of the core duplicates was not significantly different from zero ($p = 0.82$). Both the variability attributable to proximal–distal location and the variability of the core duplicates were less than the residual variability (1.1 μg/g), indicating that neither contributed much to the total variability in the bone core concentrations.

The variability (SD) of surface concentrations attributable to proximal–distal location was 1.0 μg/g ($p < 0.0008$) and that attributable to tibiae was 7.0 μg/g ($p < 0.0001$). The variability of the surface duplicates was estimated to be 0.9 μg/g ($p = 0.10$). Both the variability attributable to proximal–distal location and the variability of the surface duplicates were less than the residual variability (2.1 μg/g), indicating that neither contributed much to the total variability in the bone surface concentrations.

Modeling of core and surface tibia lead concentrations. Neither the average of the duplicate core measurements (AvgCore) nor the average of the duplicate surface measurements (AvgSurf) were normally distributed. Stem-and-leaf plots indicated that AvgCore and AvgSurf were bimodally distributed, suggesting two groups of tibiae, one with relatively high (core concentrations > 10 μg/g) and the other (tibiae 2, 3, 4, 6, 9, and 10 in Table 2) with relatively low core lead concentrations. The six tibiae in the lower group were from both sexes. AvgCore and AvgSurf measurements were normally distributed within the high and low groups. The variances of both AvgCore and AvgSurf within each location were found to be statistically homogeneous.

We used an autoregressive order (1) covariance structure, which has the desired property of having correlations that are larger for locations that are near each other, to model the correlation between measurements taken at the nine proximal–distal locations, and we used a compound symmetric covariance structure to model the correlation between AvgCore and AvgSurf measurements within a given tibia.

Table 2. Mean core and surface tibia lead concentrations (μg/g) at the midpoint and ends of dissected sections of nine adult human cadaver tibiae.

Tibia number	Proximal end (8 cm from cross-section midpoint)		Proximal–distal cross-section midpoint		Distal end (8 cm from cross-section midpoint)	
	Core	Surface	Core	Surface	Core	Surface
1	13.0	22.5	16.8	25.2	14.4	25.8
2	3.8	5.2	5.1[a]	8.5	5.4	6.4
3	6.7	11.8	8.9	14.2	8.8	16.7
4	9.0	16.5	10.3	23.0	8.2	20.2
6[b]	8.1	12.5	11.9	14.7	11.0	15.2
7	13.9	21.5	17.3	27.9	15.7	24.2
8	14.2	22.4	16.6	24.9	16.3	25.6
9	7.8	13.6	9.4	12.6	7.6	11.0
10	3.1	5.8	3.5	9.4	4.7	10.0

[a]One replicate only. [b]Tibia 5 was excluded from the analyses (see text).

In model building, a nonlinear association between tibia lead concentration and proximal–distal location was indicated by significant linear and quadratic "location" terms. The "surface, core × high, low group" interaction term was significant ($p < 0.0001$), indicating that the intercepts for the four equations (i.e., AvgCore in high-lead tibiae, AvgCore in low-lead tibiae, AvgSurf in high-lead tibiae, and AvgSurf in low-lead tibiae) were significantly different. Neither of the interaction terms, "surface, core × location × high, low group" or "surface, core × location^2 × high, low group," were significant ($p = 0.88$ and $p = 0.08$, respectively), indicating that the relationship between tibia lead concentration and proximal–distal location did not differ between the four groups with regard to rates of change (i.e., the linear and quadratic location term coefficients were not significantly different).

The final model is shown in Table 3 and Figure 2. The linear and quadratic location terms were highly significant ($p < 0.0001$) and indicate that tibia lead concentration decreased toward the ends of the tibiae for all four of the groups. Among the high-lead group, the overall difference between surface and core concentrations was 8.4 μg/g (SE = 1.3 μg/g; $p < 0.0001$; Table 4), as predicted by the model for all proximal–distal locations. Among the low-lead group, the overall difference between surface and core concentrations was 5.2 μg/g (SE = 0.9 μg/g; $p = 0.0004$; Table 4), as predicted by the model for all proximal–distal locations. Figure 2 shows that the AvgCore of the high-lead tibiae was greater than AvgSurf of the low-lead tibiae. However, the difference (3.1 μg/g) was not significant (SE = 1.9 μg/g; $p = 0.38$; Table 4). The significance of the comparison between each of the groups is shown in Table 4.

The ratio of core-to-surface lead concentrations for all locations combined is 0.64, the SD is 0.13, and the SE is 0.01.

Evidence for contiguous inhomogeneity (hot spots). When we compared locations within the same tibia for local hot spots of lead concentration, extreme studentized deviates revealed six significant differences between locations. Three of these significant differences were in the core data, and one tibia gave a significant difference between adjacent locations in both its core and its surface lead concentrations. All but one of these significant differences were part of the trend of decreasing tibia lead toward the ends of the tibiae that was observed for both core and surface tibia lead. The exception indicated a localized low core tibia lead concentration (i.e., a "cold" spot).

A test of the smallest and largest differences revealed no contiguous inhomogeneity (i.e., no hot or cold spots) in the distribution of tibia lead in either the core or the surface.

All of the differences revealed by Grubb's procedure were consistent with the trend of decreasing lead concentration toward the ends of the tibia and did not indicate any contiguous inhomogeneity in bone lead distribution.

Discussion

The cadaver tibia lead concentrations observed are consistent with the typical concentrations reported in the literature for environmentally exposed adults (*21*). It is, however, the variability within each sample that is the focus of this work. Nevertheless, our results might be applicable only to a population that is not currently exposed.

Analytical issues. Ideally, each bone sample would have been homogenized into a fine powder using a ball mill and the powdered material sampled for subsequent lead determinations. This is clearly impractical for large numbers of bone samples such as analyzed here. As an alternative, each sample was completely dissolved in concentrated nitric acid using a modified procedure based on microwave-assisted heating. Although this modified procedure was effective in homogenizing calcified bone material, complete digestion in the strictest sense, where organic matter is totally oxidized, may not have occurred. However, because the organic content of bone is quite low (i.e., principally collagen), incomplete oxidation would not be expected to be troublesome for our analytical procedure in which Zeeman-effect AAS systems can handle large amounts of background absorption. Nonetheless, the

Table 3. Model of the proximal–distal location (–8 to +8 cm) variation in core and surface tibia lead concentrations in nine adult human cadaver tibiae.

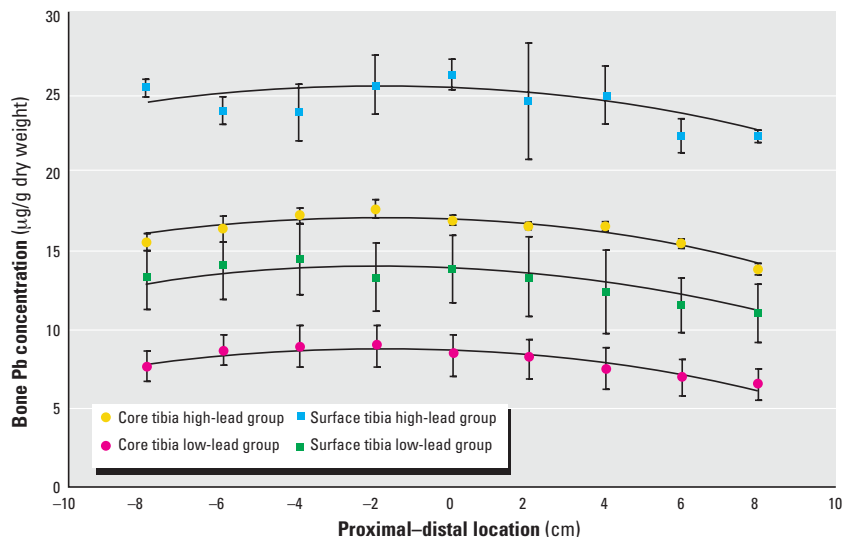| Term	Coefficient	Standard error	*p*-Value
Core tibia high-lead group intercept (μg/g)	16.9	1.4	< 0.0001
Core tibia low-lead group intercept (μg/g)	8.6	1.0	< 0.0001
Surface tibia high-lead group intercept (μg/g)	25.3	1.9	< 0.0001
Surface tibia low-lead group intercept (μg/g)	13.7	1.3	< 0.0001
(Proximal–distal location) (μg/g/cm)	–0.11	0.02	< 0.0001
(Proximal–distal location)^2 (μg/g/cm^2)	–0.028	0.004	< 0.0001

Figure 2. The proximal–distal location variability in human tibia lead concentrations measured using ETAAS with acid digestion for both core and surface tibia samples. Solid lines are the best-fit models shown in Table 3. Error bars represent the SEM of the observed concentrations.

Table 4. The differences between core and surface tibia lead concentrations in nine adult human cadaver tibiae that fell into high and low concentration groups.

Comparison	Coefficient (μg/g)	SE (μg/g)	Tukey-adjusted *p*-value
Core tibia high-lead group vs. core tibia low-lead group	8.3	1.7	0.0012
Core tibia high-lead group vs. surface tibia high-lead group	–8.4	1.3	< 0.0001
Core tibia high-lead group vs. surface tibia low-lead group	3.1	1.9	0.38
Core tibia low-lead group vs. surface tibia high-lead group	–16.7	2.1	< 0.0001
Core tibia low-lead group vs. surface tibia low-lead group	–5.2	0.9	0.0004
Surface tibia high-lead group vs. surface tibia low-lead group	11.5	2.3	0.0010

homogenization protocol was validated against NIST SRM 1400 bone ash. There was a small difference (< 0.2 μg/g) between the measured and certified concentration of the NIST SRM 1486 bone meal samples, but this difference is analytically insignificant and would not be expected to be troublesome for the analytical procedure used in this study.

Surface tibia lead concentration exceeds core tibia lead concentration. Our data suggest that surface tibia lead concentration exceeds core tibia lead concentration, independent of proximal–distal location. There are, however, few tibiae in this study, and further work would be required to more rigorously examine these observations or to examine the same questions in bones from other groups, such as children. The observation that surface tibia lead was significantly greater than core tibia lead may result from a greater bone modeling rate at the surface.

The observation that surface tibia lead concentration significantly exceeds core tibia lead concentration may render meaningless comparisons between K-shell and L-shell X-ray fluorescence measurements of lead in bone. Photon attenuation considerations dictate that LXRF samples only the superficial 1–2 mm of the tibia, whereas KXRF samples lead throughout the cross-section of the tibia (although with better detection efficiency for lead in the tibia surface). Because the actual lead concentrations are different in the core and surface of the tibia, there is little reason why LXRF and KXRF should agree. This consequence for the comparison between LXRF and KXRF says nothing about the usefulness of each in predicting biological or health outcomes.

Proximal–distal variability in tibia lead. Core and surface tibia lead decreased in a nonlinear manner toward the ends of the dissected tibia cross-sections. For completeness, it should be noted that if we assume that the tibia lead concentration is greatest at the proximal–distal midpoint of the tibia, then the midpoints of our dissected cross-sections appear to be offset from the midpoint of the entire tibia by 2–4 cm (Figure 2). It is unlikely that the decrease in tibia lead concentration toward the ends of the tibia cross-sections is an end effect because the extremities sampled were always several centimeters away from the tibia epiphyses. This observation contrasts with a report from our laboratory (*12*) that the ends of the tibia gave higher [109]Cd-based KXRF bone lead concentrations as a result of a higher degree of trabecular bone (which increases the [109]Cd-based KXRF-measured concentration) at the ends of the tibia. The effect of proximal–distal measurement location on tibia lead concentration has been examined in other studies using AAS. Wittmers et al. (*6*), in a study of human bone, reported no significant variability, but Zong and colleagues (*8,16*), who studied lead-dosed goat bones, reported an increase in lead concentration at the ends of the tibiae in some animals. This is contrary to our current observations but consistent with the [109]Cd-based KXRF observations reported previously (*12*). However, it should be reiterated that the tibia cross-sections analyzed in this report did not extend to the epiphyses, and it is possible that data from more extreme proximal and distal locations would render the location trends statistically nonsignificant.

Evidence for contiguous inhomogeneity (hot spots). One pair of measurement locations in one tibia differed in lead concentration by more than their peers; there was, therefore, the minimum possible evidence of inhomogeneity in the distribution of lead in the tibia. The localized region was one of uncharacteristically low tibia lead concentration (i.e., a cold spot). This is qualitatively consistent with a report of locally low tibia lead concentration measured by [109]Cd-based KXRF (*12*). Contiguous inhomogeneity (i.e., localized hot spots or cold spots) in the distribution of lead in tibia was not reported in previous studies using AAS (*6,8,16*). Our observation of a relatively low lead concentration may indicate that bone in this region may have lower blood flow in the Haversian canals and consequently less lead in blood available for uptake into bone during bone resorption.

Conclusion

Bone lead measurements performed on a small number of tibiae showed that lead was enriched at the tibia surface relative to the core and that lead concentrations were significantly lower toward the proximal and distal ends of the dissected tibia sections.

REFERENCES AND NOTES

1. Rabinowitz MB, Wetherill GW, Kopple JD. Kinetic analysis of lead metabolism in healthy humans. J Clin Invest 58:260–270 (1976).
2. Barry PSI, Mossman DB. Lead concentrations in human tissues. Br J Ind Med 27:339–351 (1970).
3. Barry PSI. A comparison of concentrations of lead in human tissues. Br J Ind Med 32:119–139 (1975).
4. Chettle DR. *In vivo* X-ray fluorescence of lead and other toxic trace elements. In: Advances in X-Ray Analysis, Vol 38 (Predecki P, ed). New York:Plenum Press, 1995;563–572.
5. Somervaille LJ, Chettle DR, Scott MC, Tennant DR, McKiernan MJ, Skilbeck A, Trethowan WN. In vivo tibia lead measurements as an index of cumulative exposure in occupationally exposed subjects. Br J Ind Med 45:174–181 (1988).
6. Wittmers LE Jr., Wallgren JE, Alich A, Aufderheide AC, Rapp GR Jr. Lead in bone. IV. Distribution of lead in the human skeleton. Arch Environ Health 43:381–391 (1988).
7. Parsons PJ, Zong YY, Matthews MR. Development of bone-lead reference materials for validating *in vivo* XRF measurements. In: Advances in X-Ray Analysis, Vol 38 (Predecki P, ed). New York:Plenum Press, 1995;625–632.
8. Zong Y. Atomization, Determination and Distribution of Lead in Bone by Electrothermal Atomic Absorption Spectrometry [PhD Thesis]. Albany, NY:The University at Albany, State University of New York, 1996.
9. Woodard HQ, White DR. The composition of body tissues. Br J Radiol 59:1209–1219 (1986).
10. Todd AC, Chettle DR. *In vivo* X-ray fluorescence of lead in bone: review and current issues. Environ Health Perspect 102:172–177 (1994).
11. Todd AC. Coherent scattering and matrix correction in bone-lead measurements. Phys Med Biol 45:1953–1963 (2000).
12. Todd AC, Carroll S, Godbold JH, Moshier EL, Khan FA. The effect of measurement location on tibia lead XRF measurement results and uncertainty. Phys Med Biol 46:29–40 (2001).
13. Lindh U, Brune D, Nordberg GF. Microprobe analysis of lead in human femur by proton induced X-ray emission (PIXE). Sci Total Environ 10:31–37 (1978).
14. Jones KW, Schidlovsky G, Burger DE, Milder FL, Hu H. Distribution of lead in human bone: III. Synchrotron X-ray microscope measurements. In: In Vivo Body Composition Studies - Recent Advances, Vol 55 (Yasumura S, Harrison J, McNeill K, Woodhead A, Dilmanian F, eds). New York:Plenum Press, 1991;281–286.
15. Kingston HM, Walter PJ, Engelhart GW, Parsons PJ. Laboratory microwave safety. In: Microwave Enhanced Chemistry: Fundamentals, Sample Preparation and Applications. Washington, DC:American Chemical Society, 1997;697–745.
16. Zong YY, Parsons PJ, Slavin W. Accurate and precise measurements of lead in bone using electrothermal atomic absorption spectrometry with Zeeman-effect background correction. J Anal At Spectrom 11:25–30 (1996).
17. Littell R, Milliken G, Stroup W, Wolfinger R. SAS System for Mixed Models. Cary, NC:SAS Institute Inc., 1996.
18. Latour D, Littell R. Advanced General Linear Models with an Emphasis on Mixed Models. Cary, NC:SAS Institute Inc., 1996.
19. David HA, Hartley HO, Pearson ES. The distribution of the ratio of range to standard deviation. Biometrika 41:482–493 (1954).
20. Grubbs FE. Procedures for detecting outlying observations in samples. Technomet 11:1–21 (1969).
21. Gamblin C, Gordon CL, Muir DCF, Chettle DR, Webber CE. In vivo measurements of bone lead content in residents of southern Ontario. Appl Radiat Isotop 45:1035–1038 (1994).